Performance evaluation of coded transmission for adaptive-optics corrected satellite-to-ground laser links

Lucien Canuet, Jérôme Lacan, Nicolas Vedrenne, Angélique Rissons, Géraldine Artaud

Performance evaluation of coded transmission for adaptive-optics corrected satellite-to-ground laser links

Canuet Lucien*†‡, Lacan Jérôme†, Védrenne Nicolas‡, Rissons Angélique†, and Géraldine Artaud*
*CNES, Centre National d'Etudes Spatiales, 18, av. Edouard Belin, 31401 Toulouse Cedex 9, France
†University of Toulouse; ISAE-Supaéro; TeSA; Toulouse, France
‡ONERA, The French Aerospace Lab, Theoretical and Applied Optics Department, 92322 Châtillon Cedex, France

***Abstract*—Performance estimation of coded LEO satellite-to-ground laser transmissions partially corrected by adaptive-optics are presented. Through numerical simulations, the conjugation of adaptive-optics with a cross-layering optimization of data reliability mechanisms is investigated. The emphasis is put on the minimization of the data memories required at both the transmitter and the receiver in order to guarantee an error-free downlink.**

***Index Terms*—Free-space optical communication, Adaptive-optics, Cross layer design, Interleaved codes**

I. Introduction

For future satellite-to-ground communications link, very high throughput might be achievable at a reasonable cost assuming the use of existing single mode components developed for fiber technologies such as erbium doped fiber amplifier (EDFA). However, atmospheric turbulence degrades the injection efficiency of the incoming wave into single mode components. This leads to signal fading and channel impairments. Several mitigation strategies are considered to prevent them. The use of adaptive-optics (AO) should contribute to reduce substantially the severity of the fading at the expense of potentially complex and expensive systems if very high injection stability is required.

Therefore, to reduce the loss in useful information and to relax by the same way the specifications and cost of AO systems, numerical reliability mechanisms such as interleaving and coding techniques have to be considered. The latter introduce a degree of data redundancy, which allows a transmitted codeword to be correctly interpreted despite the loss of a significant fraction of the individual codeword elements. Nevertheless, they are usually adapted to combat randomly distributed errors rather than bursty errors that are characteristic of the free-space optical channel.

Because of the typical correlation time of such a channel -milliseconds to fractions of milliseconds- and the usually envisaged data rates -several tens of Gbps- a fading event can be much longer than several codewords. This will inevitably results in an unrecoverable loss of information. To overcome this bursty distribution of errors, symbol interleaving is mandatory. Typically, these interleavers, after disassembling every codeword will spread their individual elements with a temporal interval comparable to a characteristic duration of the channel fades. In addition to the latency inherently introduced by such a fading mitigation technique, the interleaving process may simply lead to potentially high memory sizes in the case of the free-space optical channel.

To alleviate the drawbacks induced by interleavers, reliability mechanisms at the different layers of the communication stack need to be considered. On any correlated channel, by studying the interactions between these reliability mechanisms at different layers, cross-layering strategies that allow for better overall performances may be found. Extensive work on numerical approaches to mitigate free-space optical channel impairments were conducted in the US [1], Germany [2] and Japan [3]. Yet, very few results have been published on the advantages related to potential cross-layer allocation strategies of memory as well as redundancy. Furthermore, to the best of our knowledge, no work dealing with the joint impact of AO systems and the aforementioned potential cross-layer strategies has been published so far.

The present paper emphasizes numerical results characterizing the coded performances of a communication system consisting of a combination of cross-layered data reliability mechanisms for satellite-to-ground laser links corrected by AO. In Section II we introduce a model that provides time series of single-mode-fiber (SMF) coupled flux fades after AO correction. The cross-layering strategy that we have adopted as well as the model describing the coded performance estimators evaluated are described in Section III. These models are exploited in Section IV where results regarding two distinct AO systems in a LEO downlink scenario are presented.

II. Simulation of SMF Coupled Flux Fluctuations Partially Corrected by AO

The SMF coupled flux is subjected to variations conditioned by the turbulent wave-front distortions, themselves

This work was conducted in the framework of a PhD thesis supervised by ISAE-Supaéro and ONERA, and co-funded by CNES, Airbus Defense and Space and Thales Alenia Space.

Corresponding author: Canuet Lucien (email: lucien.canuet@onera.fr).

characterized by phase aberrations as well as log-amplitude fluctuations (or scintillation). Increasing the diameter of the receiver will tend to decrease the coupled flux fluctuations thanks to aperture averaging of the log-amplitude fluctuations. However this is done at the expense of a more demanding AO system needed to partially correct phase aberrations.

A Monte-Carlo based simulation tool that models both the influences of residual phase fluctuations and aperture averaged scintillation on the coupled flux has been used to generate the AO-corrected coupled flux attenuations time series used in the present paper. This simulation tool is based upon analytical models described in more details in [4]. It assumes statistical independence between scintillation and phase effects. This is soundly justified by considering the different origins of the fluctuations of the log-amplitude and the phase. The former are mostly caused by distant turbulence, whereas the latter are mostly introduced close to ground [5].

In order to generate partially corrected phase fluctuations this simplified simulator relies on the computation of random occurrences of centered normally distributed Zernike coefficients for describing the corrected phase. The temporal correlation of the latter is induced by filtering its temporal power spectra densities. The residual phase variance characterizing the performance of the simulated AO system includes terms related to the finite number of actuators (fitting error). It also takes into account wave-front sensing precision (aliasing error) and, control-loop frequency (temporal error) that should not be neglected when considering transmission links from satellites with significant orbital velocities such as LEO-to-ground downlinks. However, because of the high optical power requested for high data rates (between 40 and 140 photons per bit [6]) and the typical timescale of evolution of the atmospheric turbulence, the influence of noise upon wave-front sensing is neglected.

Since it is widely accepted that the aperture-averaged irradiance fluctuations are log-normally distributed [7], [8] as long as one does not consider strong log-amplitude fluctuation regimes, random occurrences of the latter are obtained by generating centered normally distributed variables. Temporal correlations of the irradiance fluctuations are then induced by filtering in the Fourier domain. Finally, the AO corrected SMF coupled flux attenuation is therefore given by the product of an aperture-averaged scintillation term and a phase-related injection-losses term, assuming the independence between phase and log-amplitude fluctuations mentioned earlier.

Note that this simplified model has been compared to and validated by end-to-end simulations in [9] for the downlink scenarios presented here. It provides therefore an advantage over end-to-end simulations in terms of lower time and calculation resources needed when longer time series are required in order to accurately evaluate the performance of the system through the computation of telecommunication metrics such as packet-error rates (PER).

Using the simplified simulator described above, time series of 8000 samples over a time horizon of 2 seconds were generated. The emphasis is put in this paper on the study of two LEO-to-ground scenarios characterized by two distinct AO systems: a "medium performance" and a "low performance" system. The turbulence and wind profiles of the simulated link are given in [4]. In Table I, characteristic link as well as turbulent parameters common to both scenarios are summarized. The parameters of each AO system are given in Table II.

TABLE I
CHARACTERISTIC LINK, TURBULENT AND AO PARAMETERS OF THE LEO-TO-GROUND DOWNLINK SCENARIO

Downlink Scenario	LEO
Elevation	20 deg
Range	1584 km
Orbital Velocity	7.5 $\mathrm{km\,s^{-1}}$
Rx Aperture Diameter	25 cm
Fried Parameter	0.056 m
Rytov Log-amplitude Variance	0.135

TABLE II
SYSTEM PARAMETERS FOR THE TWO AO SYSTEMS

	Medium Perf. AO	**Low Perf. AO**
Corrected radial orders	3	2
Control loop frequency	0.8 kHz	0.5 kHz
Residual phase variance	1.3 $\mathrm{rad^2}$	2.0 $\mathrm{rad^2}$
Average coupled flux attenuation	-5.2 dB	-6.7 dB

III. CODING STRATEGY: CROSS-LAYER APPROACH

In order to improve the performance of satellite-to-ground optical transmissions, data reliability mechanisms at different levels of the communication stack can be explored. By exploiting the interactions between these reliability mechanisms at different layers, cross-layering techniques and strategies that allow for better overall performances can be implemented. More precisely, we investigate in the following a coding architecture consisting of an error correcting code (ECC) at the physical layer (PL) and an erasure code (EC) at higher layers (HL). We consider as well the impact of interleaving at both the PL and the HL. By doing so, arbitrarily small average decoded PER at the output of the HL can be obtained while limiting the sizes of the memories needed at the receiver (optical ground station) and at the transmitter (satellite).

A. Instantaneous Capacity Estimation at the Physical Layer

At the receiver PL, the transmission performance is characterized by the instantaneous channel capacity $C(t)$ i.e. the maximum achievable data rate that can be reliably communicated between the transmitter and the receiver at a given instant t. Assuming soft decoding, the instantaneous capacity can be estimated using the mutual information between the detected electrical current -denoted y in the following- and the logical symbols sent $x = \{\mathrm{ZERO}, \mathrm{ONE}\}$ as:

$$C(t) = \int_Y \sum_x \Pr(x) f_{y|x}(y|x) \log_2 \left(\frac{f_{y|x}(y|x)}{\sum_x \Pr(x) f_{y|x}(y|x)} \right) dy \quad (1)$$

where $\Pr(x)$ is the probability of sending a ZERO or a ONE and is equal to 0.5. The probability distribution $f_{y|x}(y|x)$

depends on the type of detector as well as the modulation considered. Assuming that, at the receiver the background illumination level is negligible, the emphasis is put here on an optically pre-amplified PIN detector using OOK modulation. The optical amplifier is mandatory in order to overcome the photodiode noise floor and improve the detection sensitivity. A single mode EDFA is considered here as the optical amplifier. After photo-detection, it is well known that the amplified spontaneous emission (ASE) induced by the EDFA generates in the electrical domain two additional beat noises referred to as signal-spontaneous and spontaneous-spontaneous beat noise. When moderately high amplifying gains are considered the ASE noise dominates other sources of noise such as shot or thermal noises. In that case the probability density functions (PDF) of the electrical signal corresponding to either a logical ZERO or ONE have been theoretically shown to be non-Gaussian [10]. If a polarization filter is used at detection, a common approximation for such PDFs is given by [11]

$$f_{y|x}(y|x=\text{ZERO}) = \frac{1}{\left(P_{\text{ASE}} R_{\text{s}} \frac{1}{M}\right)^{M}} \frac{y^{M-1}}{(M-1)!} \exp\left(-\frac{y}{P_{\text{ASE}} R_{\text{s}}} \frac{1}{M}\right) \tag{2}$$

in the case of logical ZEROs, and by

$$f_{y|x}(y|x=\text{ONE}) = \frac{1}{P_{\text{ASE}} R_s \frac{1}{M}} \left(\frac{y}{\bar{P}_1 R_{\text{s}}}\right)^{\frac{M-1}{2}} \exp\left(-\frac{y+\bar{P}_1 R_{\text{s}}}{P_{\text{ASE}} R_s \frac{1}{M}}\right) \mathrm{I}_{M-1}\left(\frac{2\sqrt{y\bar{P}_1 R_{\text{s}}}}{P_{\text{ASE}} R_s \frac{1}{M}}\right) \tag{3}$$

in the case of logical ONEs, and where R_{s}, B_{e}, B_{o} correspond respectively to the detector responsivity, the double-sided electrical bandwidth of the receiver, the double-sided optical equivalent noise bandwidth of the filtered ASE and $M = B_{\text{o}}/B_{\text{e}}$. Note that generally these theoretical PDFs are valid in the case where $B_{\text{e}} = 1/T_{\text{s}}$ with T_{s} being the symbol period of the modulation considered. The time dependent output optical power of the signal is given by $\bar{P}_1(t) = P_{\text{in}} G A_{\text{SMF}}(t)$ where P_{in} is the average power coupled into the fiber and $A_{\text{SMF}}(t)$ is the instantaneous attenuation of the AO corrected optical power coupled into the fiber. The ASE power is given by $P_{\text{ASE}} = N_{\text{sp}} h\nu(G-1)B_{\text{o}}$, where ν is the transmission frequency, h is Planck's constant and, N_{sp} and G are respectively the inversion factor and the gain of the EDFA. The parameters corresponding to the pre-amplified detector presented in this paper are summarized in Table III. In practice, time series of instantaneous capacity are computed by applying (1), (2) and (3) to the times series of SMF coupled power attenuation generated by the simplified model described in II. At the PL, to emulate the effect of an uniform convolutional interleaver at the transmitter and the associated de-interleaver at the receiver, the instantaneous channel capacity is uniformly averaged over a sliding window of size denoted "PL interleaver Length" in the following. The latter is expressed in number of intervals of the time series generated. Therefore, the physical layer memory needed at the transmitter in order to store the corresponding data is given by the product of the sliding window's size and the numbers of bits per time interval of the instantaneous capacity time series:

TABLE III
CHARACTERISTIC PARAMETERS OF THE DETECTOR

Transmission wavelength	1550 nm
Gross Data rate	10 Gbps
Optical Filter bandwidth B_{o}	100 GHz
Electrical Filter bandwidth B_{e}	10 GHz
EDFA Gain G	38 dB
EDFA Inversion Factor N_{sp}	1
PIN Responsivity R_{s}	0.8 A/W

$$\begin{aligned}\text{Tx PL memory} = \text{PL interleaver Length} \times \text{bit Rate} \\ \times \text{interval Duration}\end{aligned} \tag{4}$$

The memory needed at the receiver is equal to the transmitter's memory times the number of bits (quantization bits) required for representing the log-likelihood ratio (LLR) needed by the soft decoder. It is fixed to 5 bits:

$$\begin{aligned}\text{Rx PL memory} = \text{PL interleaver Length} \times \text{bit Rate} \\ \times \text{interval Duration} \times \text{length LLR}\end{aligned} \tag{5}$$

B. Instantaneous Packet-Error Rate Estimation at the Higher Layers

Let us assume that at the PL the transmitter sends information at a fixed coding rate (i.e. the proportion of the data-stream that is useful i.e. non-redundant) of R_0^{PL} bits/channel use. Moreover, let us consider a perfect (ECC) in the sense of Shannon's noisy channel coding theorem. This means that the decoding has an arbitrary small error probability as soon as the instantaneous channel capacity is greater than the coding rate. Because of the randomness of the propagation channel and therefore of the instantaneous channel capacity, there is a non-zero probability that $C(t)$ is in outage i.e. falls under the code rate R_0^{PL}. When such an event occurs, the PL ECC in use will not allow for an error-free decoding. The erroneous packets are then erased. Therefore, the HL work on an input stream of instantaneous $\text{PER}(t)$ that is the output of the PL. In practice, the instantaneous $\text{PER}(t)$ at the output of the PL is obtained by thresholding the time series of instantaneous capacity to either a state of complete erasure (i.e. $\text{PER}(t) = 1$) when $C(t)$ is in outage or to an error-free ECC decoding state (i.e. $\text{PER}(t) = 1$) otherwise.

At reception, prior to erasure decoding, the effect of packet convolutional interleaving/deinterleaving at the HL can be emulated again by a uniform sliding average window that slides over the time series of $\text{PER}(t)$, thus yielding a time series of interleaved HL PER denoted $\text{PER}_{\text{HL}}^{\text{intl.}}(t)$ in the following. It is assumed that the coded packet of a given erasure codeword are spread over the interleaver length. The product of the HL sliding window's size, the numbers of bits per time interval of the time series and the physical layer code rate R_0^{PL} yields

the size of the HL memory needed at the transmitter in order to store the corresponding data:

$$\text{Tx HL memory} = \text{HL interleaver Length} \times \text{bit Rate} \times \text{interval Duration} \times R_0^{\text{PL}} \tag{6}$$

The HL memory needed at the receiver is equal to the HL transmitter's memory since erasure decoding is considered:

$$\text{Rx HL memory} = \text{HL interleaver Length} \times \text{bit Rate} \times \text{interval Duration} \times R_0^{\text{PL}} \tag{7}$$

After deinterleaving at the HL, the EC is assumed to be maximum distance separable. This means that the decoding is successful as soon as $1 - \text{PER}_{\text{HL}}^{\text{intl.}}(t)$ is greater than R_0^{HL}, with R_0^{HL} denoting the EC rate. In that case, the instantaneous decoded PER at the HL output, denoted $\text{PER}_{\text{HL}}^{\text{dec.}}(t)$, is equal to zero. When $\text{PER}_{\text{HL}}^{\text{intl.}}(t)$ is lower than the EC rate, the decoder fails and $\text{PER}_{\text{HL}}^{\text{dec.}}(t) = \text{PER}_{\text{HL}}^{\text{intl.}}(t)$.

IV. Numerical Results

A. Impact of Interleaving at Higher Layers

As a final performance metric, we introduce the average of the instantaneous higher layer decoded PER, denoted $\langle \text{PER}_{\text{HL}}^{\text{dec.}}(t) \rangle$ in the following. A transmission is considered error-free as soon as the condition $\langle \text{PER}_{\text{HL}}^{\text{dec.}}(t) \rangle = 0$ is met. Moreover, let us define the global code rate of the system as the product of the PL and HL code rates:

$$R_0^{\text{GLOBAL}} = R_0^{\text{PL}} R_0^{\text{HL}} \tag{8}$$

This global code rate sets the throughput (i.e. the useful information rate) of the transmission when it is multiplied by the gross data rate (constant and fixed to 10 Gbps here, see Table III). Note that the physical layer's code rate cannot be lower than the global code rate. For the low performance AO system, Figure 1 shows the evolution of $\langle \text{PER}_{\text{HL}}^{\text{dec.}}(t) \rangle$ against the size of the HL memory allocated at the receiver side for a transmission's throughput set to 6 Gbps, a receiver PL memory of 112 Mb and, for an average required unfaded signal-to-noise ratio of 3.9 dB. The latter, denoted SNR in the remainder, is defined as $\text{SNR} = 10 \log_{10} \left(\frac{P_{\text{in}} G}{P_{\text{ASE}}} \right)$. The distinct curves characterize different proportions of PL vs HL redundancy. One can note that the horizontal curve corresponds to the case where $R_0^{\text{PL}} = R_0^{\text{GLOBAL}}$ and therefore $R_0^{\text{HL}} = 1$ i.e. no HL erasure coding is implemented and the global redundancy is fully allocated to the PL ECC. In that case it is obvious that the HL interleaving cannot have an impact on the mitigation of fades. While $\langle \text{PER}_{\text{HL}}^{\text{dec.}}(t) \rangle$ is seen to decrease when the PL ECC code rate as well as the HL interleaver memory size increases, it seems that an optimum with respect to the PL code rate can be found. For instance, for $R_0^{\text{PL}} = 0.8$ an error-free transmission is possible when a 2200 Mb HL interleaver is used whereas for a lower PL code rate $R_0^{\text{PL}} = 0.7$, and a greater one $R_0^{\text{PL}} = 0.9$, it is not. Hereinafter, considering jointly the impact of interleaving and coding at both the PL and HL as well as the impact of the two AO system's performance presented in II, such optimums are presented.

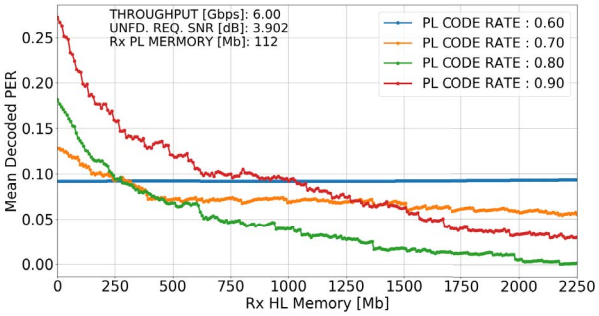

Fig. 1. Evolution of the average decoded PER against the size of the HL interleaver memory in function of the PL ECC code rate in the case of the low performance AO, a 6 Gbps throughput, a 112 Mb PL memory and, a 3.9 dB SNR.

B. Minimum Receiver and Transmitter Memories Ensuring an Error-free Transmission

The overall system under study presents numerous objective variables that can potentially be optimized over constrained ranges of several distinct parameters. As an objective variable, we focus hereafter on the minimum total memory required for an error-free downlink. That is, we have searched for the minimums $\text{Rx\_memory}_{\text{min}} = \min(\text{Rx HL memory} + \text{Rx PL memory})$ at the receiver and, $\text{Tx\_memory}_{\text{min}} = \min(\text{Tx HL memory} + \text{Tx PL memory})$ at the transmitter allowing for $\langle \text{PER}_{\text{HL}}^{\text{dec.}}(t) \rangle = 0$. Such an optimization was conducted for several throughput ranging from 5 to 7 Gbps (i.e. for global code rates ranging from 0.5 to 0.7). Arbitrary constraints were put on the SNR, the PL interleaver Length, the HL interleaver Length and R_0^{PL}. The former was allowed to range from 5.9 to 8.9 dB. PL and HL interleavers ranged respectively from 12.5 Mb to 142.5 Mb and, from 12.5 Mb to 3755 Mb. Remember that these values need to be multiplied by the number of quantization bits (5 bits here) for the receiver PL interleaver and by R_0^{PL} for both the receiver and transmitter HL interleavers in order to yield the corresponding effective memory sizes. PL interleaving is intrinsically more efficient than its HL counterpart. Therefore, here, the optimization constraints were arbitrarily biased in favor of HL interleaving (greater maximum memory allowed). Moreover, PL interleaving usually requires dedicated hardware whereas the memory allocated to HL interleaving can be in practice implemented digitally using for instance the Tx or Rx's RAM (random-access memory) which is generally not exclusively meant for that purpose. This can potentially lead to a decrease in implementation complexity that is of interest especially at the satellite's end. Finally, the largest R_0^{PL} allowed was set to 0.95.

Figures 2 and 3 show respectively the evolution of $\text{Rx\_memory}_{\text{min}}$ and $\text{Tx\_memory}_{\text{min}}$ against the throughput for the mean-normalized coupled flux attenuation corresponding to both AO systems (see Table II). This normalization is adopted in order to emphasize on the ability of AO systems to mitigate the coupled signal fluctuations just as the numerical

interleavers do. In that regard, compensating the impact of the two distinct AO systems on the average coupled flux is needed. For every point on these curves are reported the corresponding: required SNR, distribution of PL and HL code rates as well as PL and HL memories.

These results show unsurprisingly that as the throughput is increased, $\text{Rx\_memory}_{\text{min}}$ and $\text{Tx\_memory}_{\text{min}}$ increase as well. Furthermore, it is observed that on the receiver side, compared to the low performance system, the medium performance AO system permits an 85% decrease of the required memory for every throughput. At the transmitter, roughly a 95% decrease is enabled.

For the low performance AO system, the results are identical for both the receiver and the transmitter: for every throughput considered the $\text{Rx\_memory}_{\text{min}}$ and $\text{Tx\_memory}_{\text{min}}$ are found for the highest SNR allowed. At the physical layer, R_0^{PL} can be seen to increase with the throughput while no memory is allocated for interleaving at this layer. Instead it is distributed entirely to the HL where R_0^{HL} does not necessarily increase with the throughput.

In the contrary, for the medium performance AO system, the results at receiver differ from those at the transmitter. At the receiver the trends are comparable to those regarding the low performance AO system: the optima are always found for the highest SNR while R_0^{PL} increases with the throughput and, R_0^{HL} varies without a notable trend. The memory is again entirely allocated to the HL. However, on the transmitter side the global redundancy is entirely allocated to the PL (i.e. $R_0^{\text{PL}} = R_0^{\text{GLOBAL}}$) and there is therefore no HL coding. In consequence the memory is also entirely distributed to the PL. Note as well the interesting feature characterizing the relation between the PL memory and the SNR: successively, as the throughput increases, the PL memory can be kept constant while the SNR increases slightly and vice versa.

Assuming that one seek to minimize the overall memory resources required by the system, these results highlight mainly two features. When facing challenging turbulent conditions, the global redundancy of the system should be distributed to both the PL and the HL while its memory should be distributed entirely to the HL. When the turbulent conditions are less severe, it might be more advantageous to completely allocate both the redundancy and the memory to the PL. Note that this is true for the case considered here where a greater memory for interleaving was allowed on the HL than on PHY.

V. Conclusion

In this paper, simulation results assessing the performance of coded LEO-to-ground laser transmissions are presented. The impact of AO correction combined with a cross-layer optimization of numerical reliability mechanisms including physical layer error correcting codes, higher layer erasure code and interleaving at both layers has been exposed. It is shown that by exploiting the interactions between these distinct reliability mechanisms better overall performance can be achieved. In particular, the global data memory required by the interleavers at the receiver and on the satellite can be minimized while providing an error-free transmission. Finally, in addition to drastically reducing the aforementioned memories, it is shown that the use of better AO systems can have an impact on the optimal distribution of redundancy and interleaving memory over the physical and higher layers.

References

[1] X. Zhu and J.M. Kahn, "Performance bounds for coded free-space optical communications through atmospheric turbulence channels," IEEE Transactions on communications, Vol. 51, No. 8, August 2003.

[2] Henniger, Hennes, "Packet-Layer Forward Error Correction Coding for Fading Mitigation," In: Proceedings of SPIE – Volume 6304, 630419-1-630419-8. SPIE Optical Press. Free-Space Laser Communications VI, 2006-08-15 -2006-08-17, San Diego, California, USA. ISBN 0-8194-6383-3. ISSN 0277-786X.

[3] Takenaka, H., Okamoto, E., and Toyoshima, M., "Low-density generator matrix code for correcting errors with a small optical transponder," In IEEE International Conference on Space Optical Systems and Applications, 2015, pp. 1-4.

[4] N. Vedrenne and J.-M. Conan and C. Petit and V. Michau, "Adaptive optics for high data rate satellite to ground laser link," In Proc. SPIE 9739, Free-Space Laser Communication and Atmospheric Propagation XXVIII, 97390E, 2016

[5] N. Perlot, "Turbulence-induced fading probability in coherent optical communication through the atmosphere," Appl. Opt., 29, pp 7218–7226, OSA, vol.46, October 2007.

[6] Fidler, F. and Knapek, M. and Horwath, J. and Leeb, W. R., "Optical communications for high-altitude plat-forms," IEEE, vol. 16, 2010.

[7] Tatarski, V.I., Wave Propagation In a Turbulent Medium, Dover Publications,Inc. New York, 1961.

[8] Strohbehn, J. W., Laser Beam Propagation in the Atmosphere, Springer Berlin Heidelberg, 1978.

[9] L. Canuet, N. Védrenne, J-M. Conan, C. Petit, G. Artaud, A. Rissons, and J. Lacan "Statistical properties of single-mode fiber coupling of satellite-to-ground laser links partially corrected by adaptive optics," unpublished.

[10] P. A. Humblet and M. Azizoglu, "On the bit error rate of lightwave systems with optical amplifiers," in Journal of Lightwave Technology, vol. 9, no. 11, pp. 1576-1582, Nov 1991.

[11] B. Chan and J. Conradi, "On the non-Gaussian noise in erbium-doped fiber amplifiers," in Journal of Lightwave Technology, vol. 15, no. 4, pp. 680-687, Apr 1997.

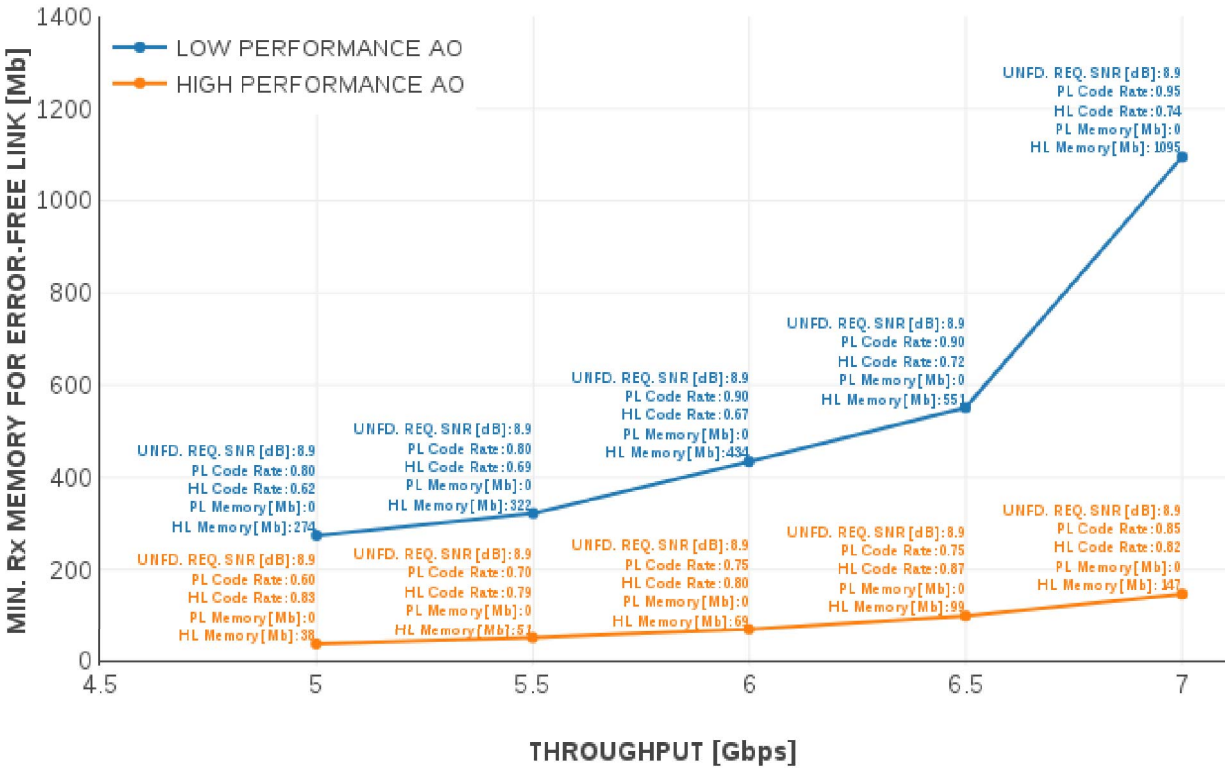

Fig. 2. Evolution of the minimum total memory of the receiver allowing an error-free transmission against the throughput.

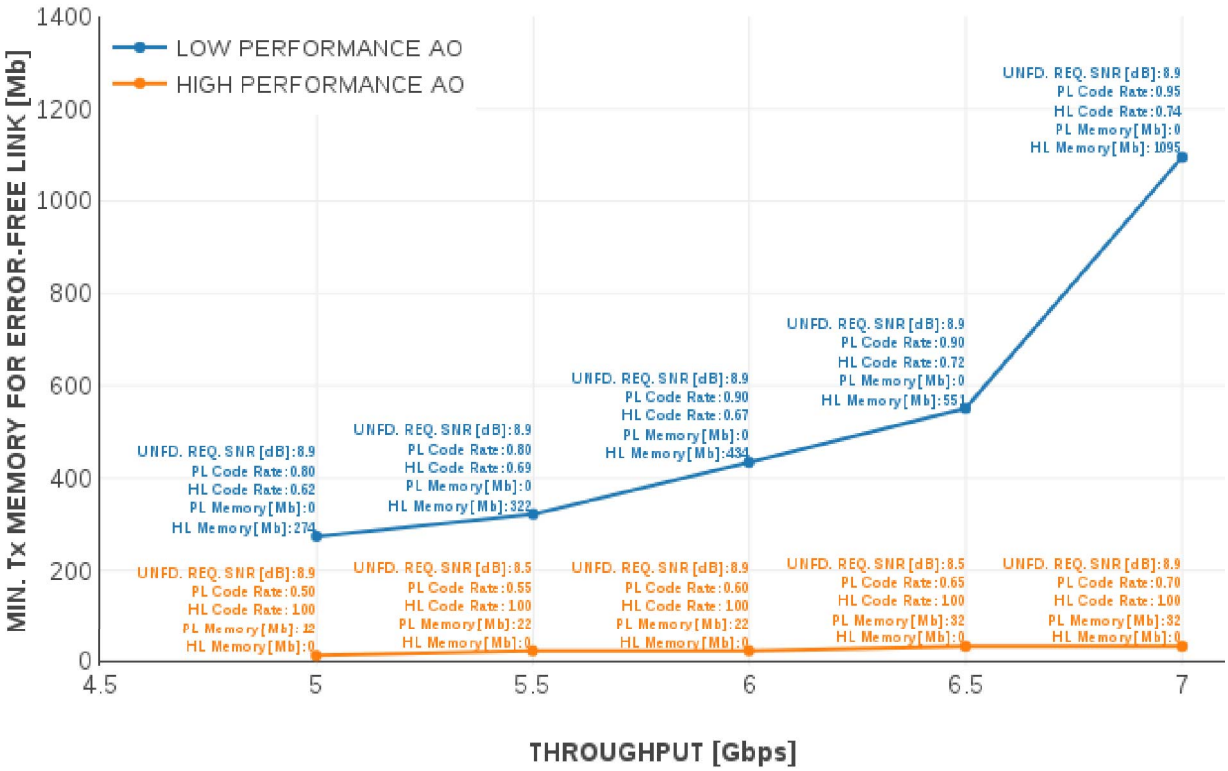

Fig. 3. Evolution of the minimum total memory of the transmitter allowing an error-free transmission against the throughput